ISSN 0015-4628, Fluid Dynamics, 2010, Vol. 45, No. 2, pp. 312–324. © Pleiades Publishing, Ltd., 2010.
Original Russian Text © V.V. Vedeneev, S.V. Guvernyuk, A.F. Zubkov, M.E. Kolotnikov, 2010, published in Izvestiya Rossiiskoi Akademii Nauk, Mekhanika Zhidkosti i Gaza, 2010, Vol. 45, No. 2, pp. 161–175.

Experimental Investigation of Single-Mode Panel Flutter in Supersonic Gas Flow

V. V. Vedeneev, S. V. Guvernyuk, A. F. Zubkov, and M. E. Kolotnikov

Received September 3, 2009

Abstract—Panel flutter theory distinguishes between two types of the loss of stability, namely, the flutter of the coupled type and the single-mode flutter. The flutter of the coupled type is well studied, both theoretically and experimentally. The single-mode flutter has been theoretically studied only quite recently. This study is devoted to the experimental investigation of the single-mode panel flutter. The fact of its generation under actual conditions is established and the stability range is determined.

DOI: 10.1134/S001546281002016X

Keywords: panel flutter, plate flutter, high-frequency flutter, single-mode flutter, flutter with one degree of freedom.

Panel flutter is an aeroelastic phenomenon leading to fatigue damages of flight vehicles. Let us consider a skin panel of a flight vehicle in supersonic gas flow; for example, Fig. 1 presents a wing skin. If the flight velocity is not too high, then the static equilibrium position of the panel is stable. However, if a critical Mach number M_{cr} is exceeded, the panel loses stability and begins to vibrate. The vibrations are due to energy supply from the flow to the panel and can be of large amplitude, thus leading to fatigue damages of the flight vehicle skin and the associated design elements.

The problem of skin panel flutter presented itself in the forties of the last century and has a rich research history. The theory consists in the solution of an eigenvalue problem for the coupled panel/flow system. We will assume that the panel is a flat elastic plate oscillating in accordance with the harmonic law $w(x,\ t) = W(x)e^{-i\omega t}$ (for simplicity we will consider only the two-dimensional formulation of the problem); then the equation of motion of the plate takes the form:

$$D\frac{\partial^4 W}{\partial x^4} - \omega^2 W + p\{W,\ \omega\} = 0, \tag{0.1}$$

where D is the plate rigidity and $p\{W,\ \omega\}$ is the flow pressure acting on the plate. The accurate theory of potential gas flows gives expression [1], which, having been substituted in Eq. (0.1), leads to a complicated integro-differential equation. Considerable advances in its investigation were made in the fifties of the last century, when the piston theory formula was derived. It represents a simple approximation for the gas pressure, valid for high Mach numbers

$$p\{W,\ \omega\} = \frac{\mu \mathrm{M}}{\sqrt{\mathrm{M}^2 - 1}}\left(-i\omega W(x) + \mathrm{M}\frac{\partial W(x)}{\partial x}\right). \tag{0.2}$$

The main advantage of the piston theory is that it replaces a complicated integro-differential equation of plate oscillations in a gas flow by a simple partial differential equation which can be investigated numerically and even analytically. For many years the piston theory has served as the main tool in studying supersonic aeroelasticity problems. Usually, all generalizations of the panel flutter problem were related with the "elastic" part of the problem, while the gas flow action was calculated using Eq. (0.2). Among a great many studies only a few authors used potential flow theory or more general theories [2–10].

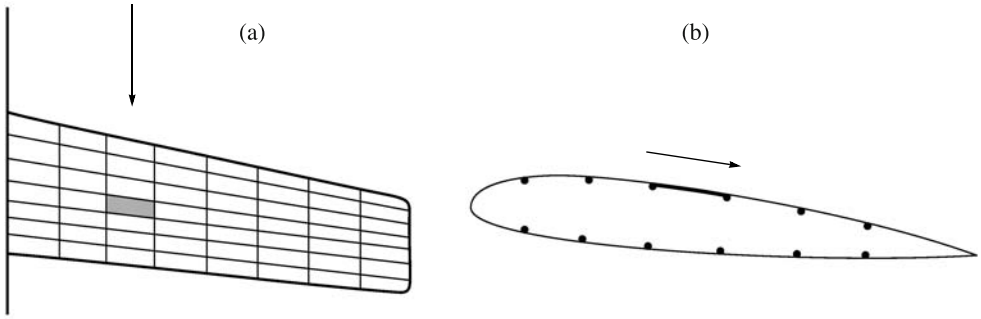

Fig. 1. Wing skin panel as a typical structure undergoing panel flutter.

However, despite its advantages, the piston theory has an important shortcoming, since it is capable of describing only one mode of possible panel flutter mechanisms. Two types of panel flutter are known. The first is the coupled-type flutter due to the interaction between the plate eigenmodes. It is completely amenable to the treatment using the piston theory which gives good agreement with experimental data for $M > 1.7$. The second is the single-mode flutter which is also referred to as high-frequency flutter. This can be detected only by means of potential flow theory or more general theories. Until recently, it is only in a few studies [2, 4, 6], in which the problem was numerically solved, that possible occurrence of the single-mode flutter under certain conditions was mentioned but the physical mechanism of the loss of stability was not investigated. A detailed study of the flutter of this type has not been carried out; moreover, its actual existence itself has been subjected to question. In the last few years the single-mode flutter was studied in detail in [11–15], where, moreover, a simple physical mechanism of its generation was revealed. So far, the single-mode flutter has not been studied in experiments.

This study is devoted to experimental detection of the single-mode flutter. The experiments were performed in a supersonic A-7 wind tunnel of the Institute of Mechanics of the Moscow State University. The main element of the experimental model was an elastic plate fastened along its perimeter and so chosen that the coupled-type flutter could occur under no circumstances, whereas the single-mode flutter could take place. In the process of the experiment plate oscillations, pressure fluctuations, and tunnel vibrations were monitored. An analysis of these data made it possible to study the mode of the oscillations that were excited.

1. DESCRIPTION OF THE EXPERIMENTS

The model consisting of a rigid frame and a steel plate measuring $500 \times 300 \times 1$ mm welded on the frame along the perimeter was mounted on the wall of the wind tunnel, as shown in Fig. 2a (the short side of the plate is aligned with the flow). Beneath the plate there was a cavity communicating with the flow region in the tunnel via bypass channels, so that the pressure in the cavity was equal to the static pressure in the flow. As a result, the plane state of the plate was its equilibrium position about which it could freely oscillate.

Twelve strain gages were cemented to the cavity side of the plate in order to record its oscillations; these were connected with a 24-channel ATM/D24 amplifier that ensured the measurement of the dynamic component of a signal on the range from 20 to 10,000 Hz.

An AR2037 vibration detector complete with an AS02 converter was used to monitor the tunnel vibrations. The detector was mounted on the wall of the test section of the tunnel, near the model.

The measurement procedure is schematically shown in Fig. 3. Signals on the outputs of the ATM/D24 strain-measuring equipment and signals from the vibration detector were recorded in parallel using a *Mera* MIC300-M system (recorder) and a *National Instruments* personal computer with a PCI-6013 analog-digital plate monitored by the LabVIEW software. The polling frequency of the recorder was 13 kHz and that of the computer was 10 kHz. The MIC300-M recorder was also used for monitoring in real time the dynamic stress level in the plate in the course of an experiment.

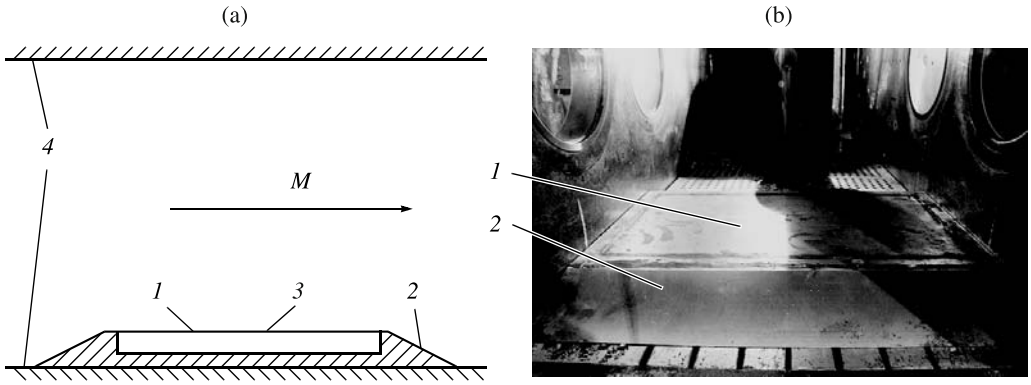

Fig. 2. Schematics of the experiment (a): (*1*) plate; (*2*) frame; (*3*) cavity; and (*4*) tunnel walls. Model as an assembly mounted in the wind tunnel (b).

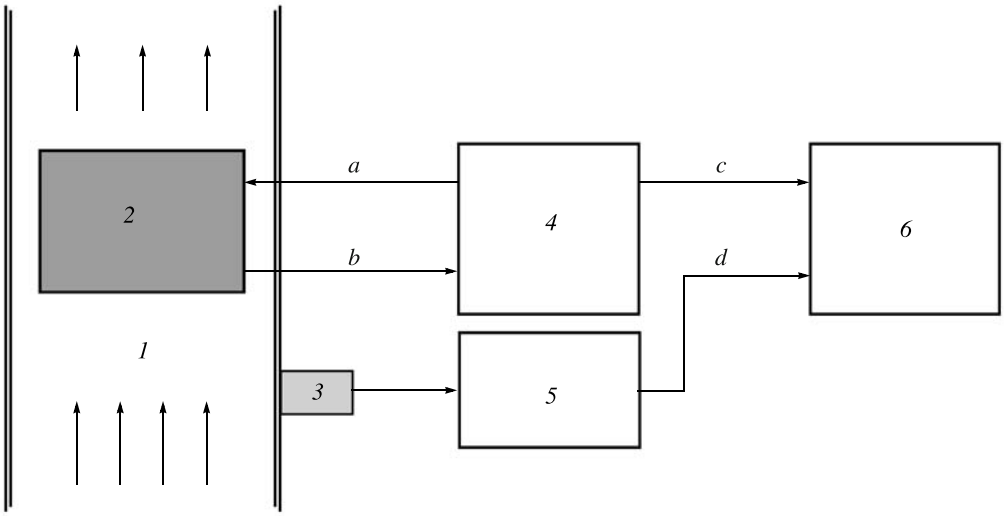

Fig. 3. Schematics of the measurement procedure (pressure transducer is not shown). (*1*) wind tunnel; (*2*) plate with strain gages; (*3*) AP2037 vibration detector; (*4*) ATM/D24 strain-measuring equipment; (*5*) AS02 converter; and (*6*) *Mera* MIC300-M recorder. Connectings: *a* strain gage power; *b* strain gage signal; *c* strain gage signal (output); and *d* vibration detector signal.

The design flow parameters in the tunnel were monitored using standard pressure gages. A *Honeyweel* 186PC15DT transducer with the polling frequency of 10 kHz was used for measuring pressure fluctuations.

In the course of our experiments performed in transonic tunnel operation regimes (M = 0.8 to 1.3) the typical values of the physical parameters of the air in the plenum chamber were as follows: the specific heat ratio $\gamma = 1.4$, the total pressure $p_0 = 112$ to 142 kPa, and the stagnation temperature $T_0 = 286$–279 K.

Generally, during the tunnel operation plate vibrations of five types can be generated. These are resonance oscillations supported by either tunnel wall vibrations or pressure fluctuations in the flow, a response to broadband noise occurring during tunnel operation, flutter oscillations of the coupled type, and single-mode flutter oscillations.

Since the purpose of the experiments was to reveal single-mode flutter oscillations, they need to be identified among oscillations of other types. The idea of the identification consists in breaking down the investigation into the following stages.

First, the spectra of plate oscillations, tunnel wall vibrations, and pressure fluctuations in the flow are analyzed. If, as a result of the measurements, the plate oscillations are found to contain some frequencies which are absent from the tunnel vibration and pressure fluctuation spectra, then these oscillations cannot be a resonance caused by the tunnel vibrations or the pressure fluctuations.

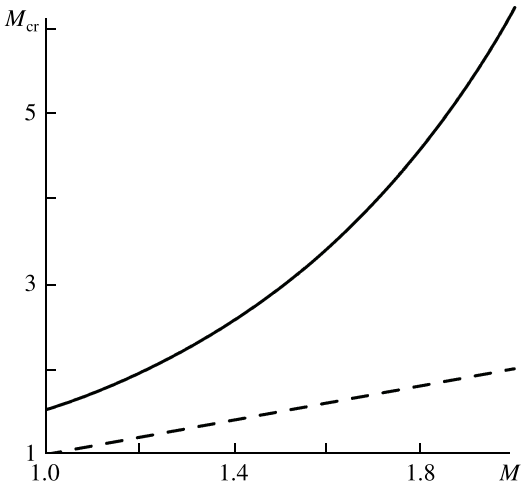

Fig. 4. $M_{cr}(M)$ curve in accordance with Eq. (4.1). The broken line corresponds to $M_{cr} = M$.

To reveal plate oscillations that represent its response to broadband noise of the tunnel the dependence of the plate oscillation amplitude on the tunnel vibration amplitude is analyzed in several regimes. If in certain regimes the plate oscillation amplitude increases, whereas the tunnel vibration amplitude increases more slowly, or remains unchanged, or even decreases, then the plate oscillation amplification cannot be due to a response to broadband noise.

The coupled-type flutter can be separated from oscillations of other types using the fact that before it has occurred the frequencies of the (1, 1) and (2, 1) modes must close together (here, (m, n) is considered to mean the mode having m half-waves of the natural form of deflection in the flow direction and n half-waves in the perpendicular direction). If the coalescence of the corresponding peaks in the spectrum is not observable with increase in the Mach number M, then the oscillations cannot be the coupled-type flutter.

If all forms of forced oscillations and the coupled-type flutter are excluded, then the remaining oscillations in accordance with the theoretically predicted forms should be recognized to be the single-mode flutter.

We will make a note about the Mach number values presented below. The equipment used in our experiments makes it possible to determine the value of M accurate to 0.01. Nevertheless, by means of multiple repeated measurements we were able to distinguish with certainty between transonic flow regimes differing from one another with respect to the "formal" Mach number by a value of the order of 0.001. Thus, in the cases in which the Mach number values presented below are given to the third decimal place it should be understood in the relative meaning, that is, as an indicator of different tunnel operation regimes, though the characteristic physical Mach number cannot be displayed more accurately than to the second decimal place.

2. EXPERIMENTAL PROGRAM

The experiments were conducted in the A-7 wind tunnel operating in transonic and supersonic regimes. Altogether, three runs were carried out, namely, two runs with continuous variation of the Mach number from 0.8 to 1.3 and a run with $M = 3$.

Before every tunnel startup all measurement systems were tested against their fitness for work (the responses of all the strain gages and the vibration detector to accentuated knocks on the plate and the tunnel walls were recorded) and the natural frequencies of the free oscillations of the plate were determined.

In the transonic regime ($0.8 < M < 1.3$) the Mach number was varied by means of stepwise adjustment of the pressure level in the plenum chamber of the tunnel. During one run it was possible to realize five constant regimes, 10–15 s in duration. During the first run it was the regimes with the nominal Mach numbers $M = 0.857$, 1.167, 1.286, 1.292, and 1.298 and during the second run the regimes with $M = 1.169$, 1.147, 1.285, 1.294, and 1.293. For $M = 3$ the constant regime duration was 60 s. During each run the readings of all the transducers were continuously and synchronously recorded.

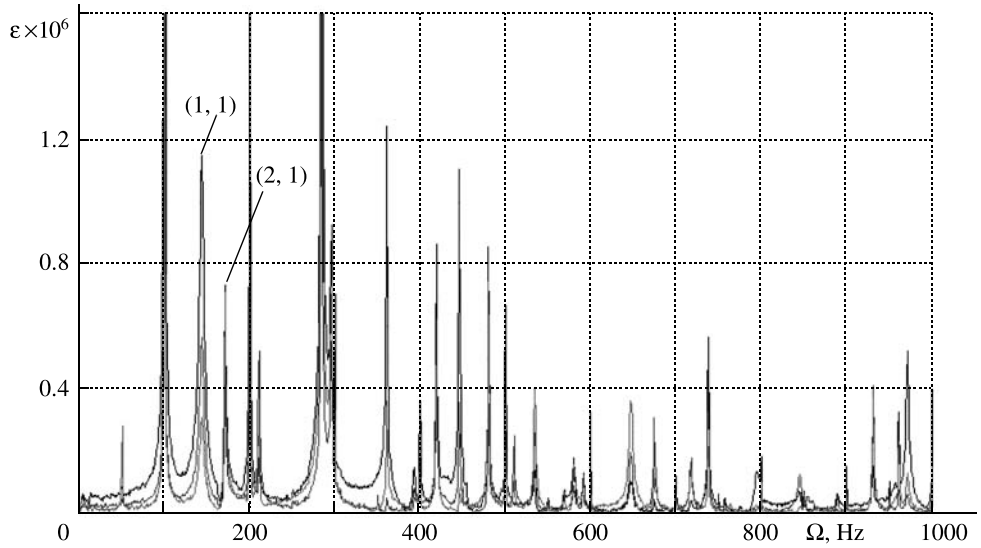

Fig. 5. Spectrum of the natural oscillations of the plate stroked at the center.

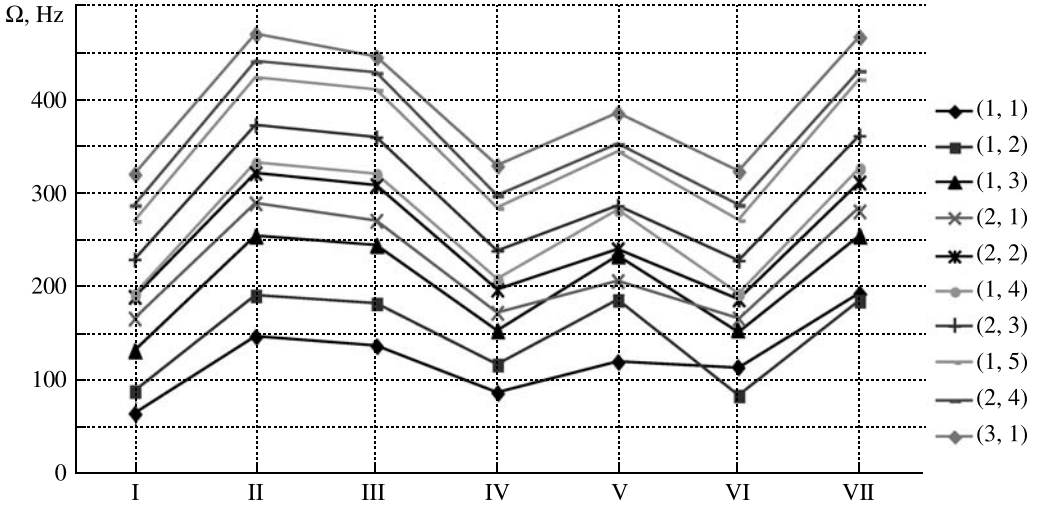

Fig. 6. Influence of various factors on the natural frequencies of the plate. Flat plate (I); flat plate, $T = -5°$C (II); bulged plate with an amplitude of 1 mm, $T = -5°$C (III); bulged plate with an amplitude of 1 mm (IV); bulged plate with an amplitude of 3 mm (V); flat plate with account for the cavity (VI); and flat plate with account for the cavity, $T = -5°$C (VII).

Thus, the plate oscillations were recorded in 10 regimes on the transonic range of the wind tunnel operation and in one supersonic regime.

3. TECHNIQUE OF PROCESSING THE RESULTS

After the experiments have been completed, the records of the plate deformations, the tunnel vibrations, and the pressure fluctuations were subjected to the following analysis. In each tunnel operation regime certain regions, 5 or 10 s in duration, were separated out and the fast Fourier transformation was performed on these regions. In the amplitude-frequency characteristics thus obtained fairly strong peaks characterizing the oscillations were separated out. For each peak the temporal process was filtered out on a 5–10 Hz-wide range around the main frequency of the peak and the oscillation shape was determined from an analysis of the phase shift between different transducers and their amplitudes. As a result, for each tunnel operation regime the frequencies and shapes of the main oscillation components were determined.

These results were then compared with the results of the similar processing of the readings of the tunnel

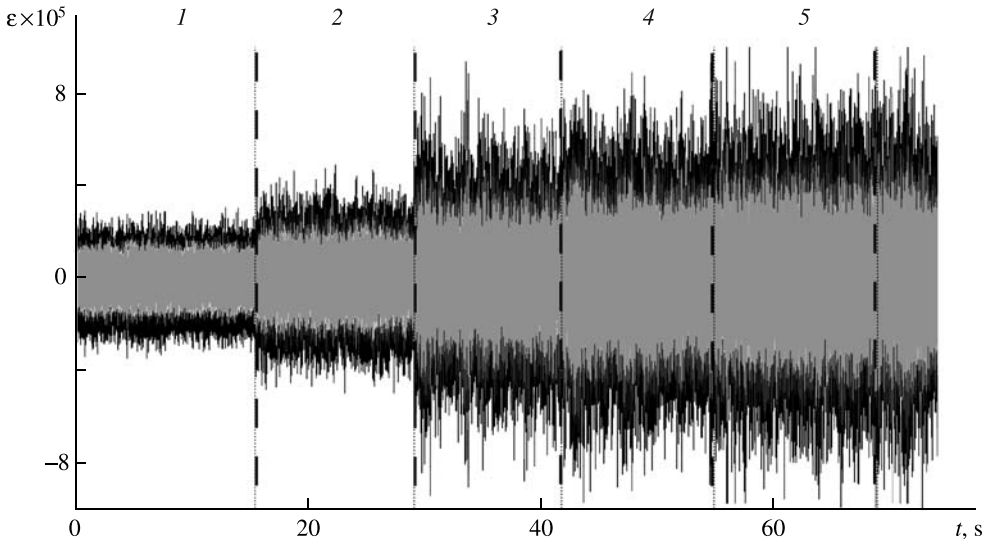

Fig. 7. Plate oscillation process during the first run. The M = 0.857, 1.167, 1.286, 1.292, and 1.298 regimes are separated by the broken lines (*1–5*).

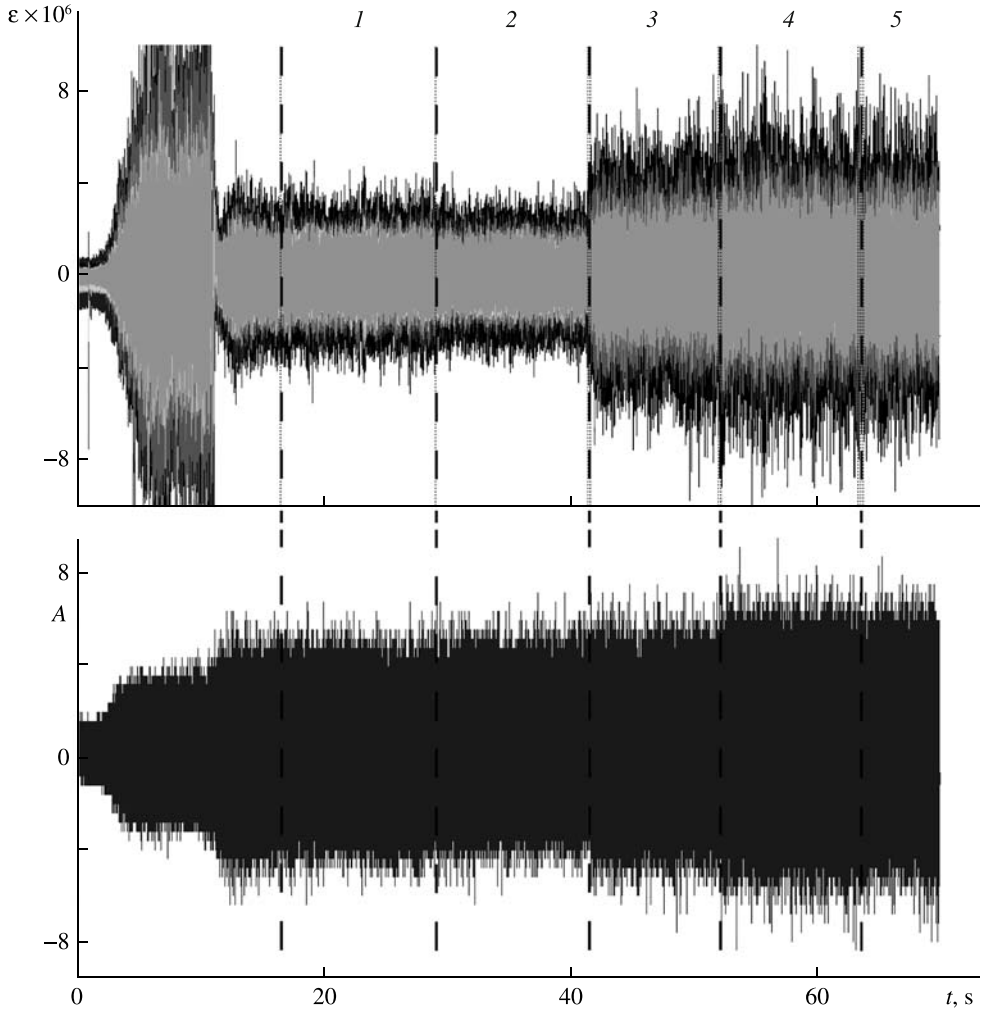

Fig. 8. Plate oscillations (a) and tunnel vibrations (b) during the second run. The stable M = 1.169, 1.147, 1.285, 1.294, and 1.283 regimes are separated by the broken lines (*1–5*).

vibration and pressure fluctuation transducers using the algorithm described above.

The experimental data were processed using the *Mera WinPOS Expert* program. The program makes it possible to carry out the real and complex Fourier transformations and to filter out a signal on a given frequency range with representation of the results in a convenient graphical form.

4. THEORETICAL CALCULATIONS

The plate dimensions were so chosen beforehand, that the "classical" coupled-type flutter could not arise in the wind tunnel used. In fact, for the coupled-type flutter the critical Mach number is given by the formula [16]

$$\mathrm{M}_{\mathrm{cr}} = \frac{D}{p\gamma L_x^3}\frac{8\pi^3}{3\sqrt{3}}\left(5 + \frac{L_x^2}{L_y^2}\right)\sqrt{2 + \frac{L_x^2}{L_y^2}}, \tag{4.1}$$

where L_x and L_y are the plate dimensions (the air flow is directed along the x axis), D is the plate rigidity, p is the static pressure in the flow, and γ is the specific heat ratio. In turn, the static pressure varies depending on the Mach number. Using the isentropic formula

$$p(\mathrm{M}) = p_0\left(1 + (\gamma - 1)\frac{\mathrm{M}^2}{2}\right)^{-\gamma/(\gamma-1)}$$

and the total pressure value p_0 typical of the tunnel used we obtain the function $\mathrm{M}_{\mathrm{cr}}(\mathrm{M})$. Formula (4.1) was derived for a hinge-supported plate, the value M_{cr} being even higher for a fixed plate. From the $\mathrm{M}_{\mathrm{cr}}(\mathrm{M})$ curve plotted in Fig. 4 for the typical experimental parameters it can be seen that for any M there holds the inequality $\mathrm{M}_{\mathrm{cr}} > \mathrm{M}$, so that theoretically the coupled-type flutter cannot occur. It was not also observable in our experiments.

Contrariwise, in accordance with the theory, the single-mode flutter must occur. In our calculations we used theory [13]. For any plate eigenmode (m, n) there exists a flutter range $\mathrm{M}_1(m, n) < \mathrm{M} < \mathrm{M}_2(m, n)$. The modes excited for $\mathrm{M} < 1.3$ are given below.

m	1	2	2	3	3	4	4
n	1	1	2	1	2	1	2
Frequency, Hz	64.7	167.5	190.4	321.4	344.3	526.4	549.4
M_1	1.19	1.17	1.28	1.20	1.26	1.25	1.29
M_2	1.56	1.48	1.61	1.48	1.54	1.49	1.53

As a result of the spectral analysis of the experimental data we obtained clearly expressed peaks in the amplitude-frequency characteristics at the following frequencies:

In the $\mathrm{M} < 1.17$ regimes excitation is absent.

In the $1.28 < \mathrm{M} < 1.30$ regimes there are peaks at frequencies 64.7 Hz (form (1, 1)), 167.5 Hz (form (2, 1)), 190.4 Hz (form (2, 2)), 321.4 Hz (form (3, 1)), 344.3 Hz (form (3, 2)), 526.4 Hz (form (4, 1)), and 549.4 Hz (form (4, 2)).

In the $\mathrm{M} = 3.0$ regime there are peaks at frequencies 192.7 Hz (form (1, 4)), 562.3 Hz (form (2, 7)), and 969.7 Hz (form (3, 9)). It should be noted that in this case the calculations of the oscillation growth rates in accordance with [13] give very small, near-zero increments for these three theoretically-excited modes, so that it might be expected that in the $\mathrm{M} = 3.0$ regime the flutter is not excited.

These results were obtained without taking account for the factors discussed in the following section. Taking them into account leads to an increase in the mode (1, 1) frequency and the displacement of the corresponding flutter range toward greater Mach numbers, whereas the frequencies of the other modes and the corresponding flutter ranges change only slightly if at all.

5. NATURAL OSCILLATIONS OF THE PLATE

For the purpose of verifying the dynamic properties of the model we performed previously an experiment on the determination of the natural frequencies and forms of the oscillations by means of accentuated stroke on the plate. To reveal all the forms and to exclude the possibility that the stroke zone may fall on the node line of one or another form we made several strokes on the center of the plate and its corners, whereupon we chose two strokes of most informative type (one on the center and one on a corner), at which the greatest number of the eigenmodes could be excited.

For the spectral analysis we chose 2 s-long signal intervals. The natural frequencies detected on the stroke on the center are shown in Fig. 5. All the peaks multiple to 50 Hz (50, 100, 150, 200 Hz, etc.) represent noises of the supply line. One can assure himself that this is the case by filtering out the signal near any of these peaks and discovering that the oscillations do not take the form of standing waves.

From the standpoint of flutter the most important modes are (1, 1) and (2, 1). The experimentally determined frequencies are as follows: 143 Hz for the (1, 1) mode and 170 Hz for the (2, 1) mode. The classical formula for the natural frequencies of a fixed plate gives 65 Hz for the (1, 1) mode and 167 Hz for the (2, 1) mode. Thus, we obtain good agreement between the theory and the experiment for the (2, 1) mode and disagreement for the lower (1, 1) mode.

In order to understand the reason for this disagreement we studied the effect of three factors on the dynamic properties of the model by means of numerical modeling using the ABAQUS software. These factors, which were not adequately controlled in the experiments, are the presence of air in the cavity, the temperature, and residual stresses in the plate. We will consider them in order.

The first factor is the presence of the cavity beneath the plate, which could be imperfectly communicated with the flow thus forming a kind of an "aerodynamic spring" at symmetric oscillation modes and leading to an increase in the frequency of the natural oscillations of the plate. In this case, the air closed in the cavity has no effect on the antisymmetric-mode oscillations.

The second factor is the plate temperature influence on the oscillation frequencies. During the tunnel startup, when the flow temperature is strongly different from the initial temperature of the plate surface, the thin plate is cooled more rapidly than the massive frame. The tension thus generated leads to an increase in the natural frequencies.

Finally, the third factor which was not subjected to quantitative checking, is the presence of residual stresses in the plate, which could arise when it had been welded to the frame. The plate had a certain initial curvature (bulge) which was directly modeled in the numerical analysis.

Figure 6 presents the corresponding results for several first frequencies. Clearly, the only calculated case in which the natural frequencies of the (1, 1) and (2, 1) modes are similar to those detected in the experiments is the case VI of a flat plate with account for a cavity and without temperature stresses.

From the standpoint of flutter the variations in the natural frequencies (at invariant bending shapes) can be taken into account using the following equation for calculating the lower (in the Mach number) boundary of the flutter range [13]

$$\mathrm{M}_1 = \frac{1 + (C/a(\mathrm{M}_1))}{\cos\alpha},$$

where $a(\mathrm{M})$ is the speed of sound in the flow and C is the phase velocity of the waves forming the eigenfunction [13]. The angle α is determined by the bending shape; for the expected flutter forms it is given below.

m	1	2	2	3	3	4	4
n	1	1	2	1	2	1	2
α, deg	24.6	13.9	26.7	9.72	19.0	5.4	14.7

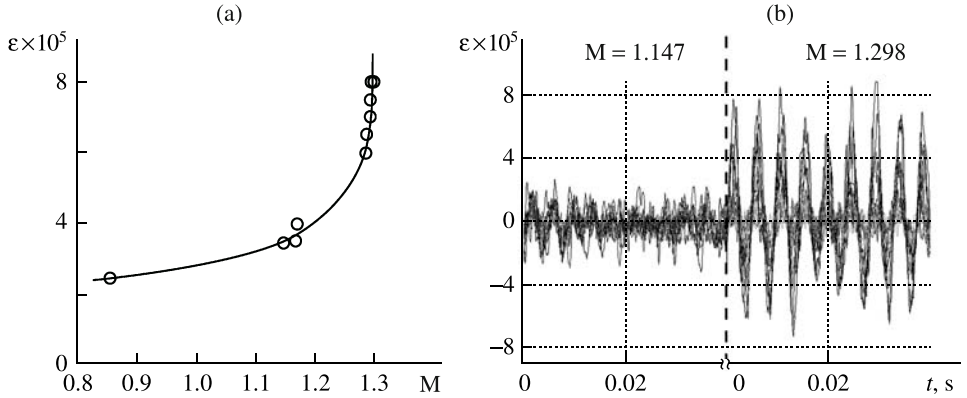

Fig. 9. Plate oscillation amplitude as a function of the Mach number (a). The points are the experimental data and the line is the interpolation of the values obtained. Plate oscillations in M = 1.147 (stable process) and M = 1.298 (flutter) (b).

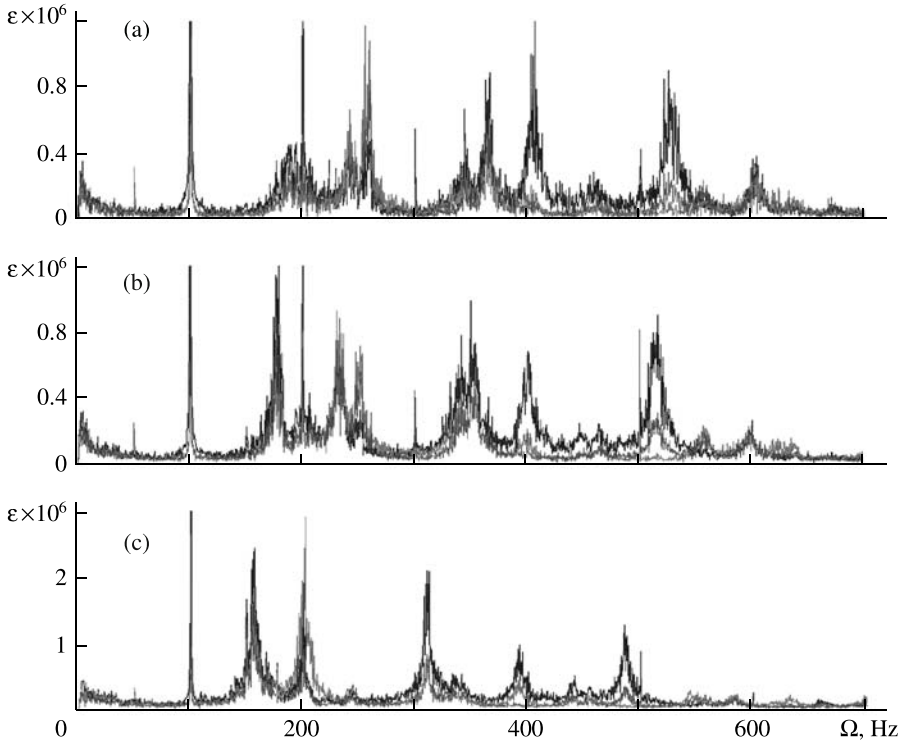

Fig. 10. Plate oscillation spectra in the M = 1.147, 1.167, and 1.286 regimes (a–c).

6. RESULTS OF THE EXPERIMENTS

We will first consider transonic regimes of tunnel operation. Before analyzing the oscillation spectra we will present the types of the processes recorded in accordance with the data of the pressure gages and the vibration detector (Figs. 7 and 8). In view of the fact that the vibration detector did not function during the first run, the corresponding data are absent.

In Fig. 9a we have plotted the plate oscillation amplitude against the Mach number from the data of runs 1 and 2. Clearly, starting from M ≈ 1.2 the amplitude begins to increase sharply, though the tunnel vibrations increase only by about 30%.

In Fig. 9a the amplitudes were calculated as the greatest mean amplitudes of three successive peaks in the oscillation process. Actually, this is the maximum amplitude realized during tunnel operation in the given regime, which cannot be regarded as an accidental interference. These amplitudes were reached only rarely. The "actual" amplitudes realized on the average in each oscillation cycle were 1.5 to 2 times lower

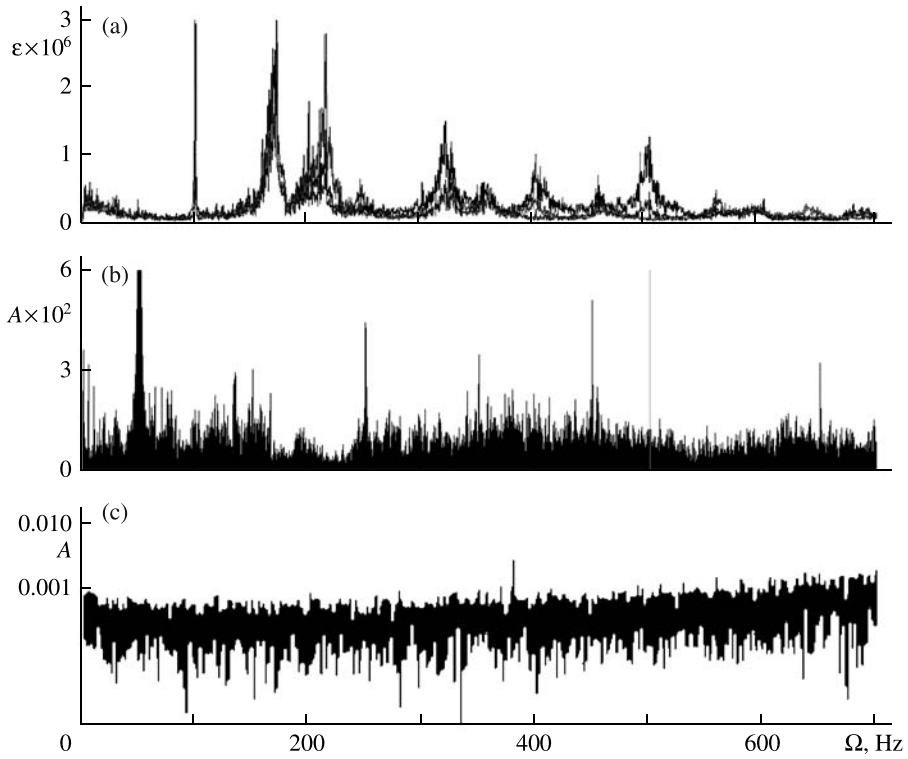

Fig. 11. Plate oscillation spectrum in the M = 1.147 regime (a), typical tunnel wall vibration spectrum (b), and typical pressure fluctuation spectrum (c).

(Fig. 9b); however, if a similar curve would be plotted for these amplitudes, the tendency toward an increase in the amplitude with the Mach number remains obviously the same.

Since the recordings were partially made in close regimes with almost identical data obtained, we will choose for the spectral analysis the following sequence of the regimes and time intervals: M = 0.857, 1.147, 1.167, 1.286, and 1.298.

The spectra obtained in these regimes are presented in Figs. 10 and 11a. Here and in what follows, all the peaks with frequencies multiple to 50 Hz are electrical interferences and for this reason are ignored.

The tunnel vibration spectrum remains almost invariant in different transonic regimes and represents broadband noise with no expressed peaks. By way of illustration, in Fig. 11b we have presented the tunnel vibration spectrum in the M = 1.294 regime. The pressure fluctuation spectrum shown in Fig. 11 also represents broadband noise.

We will consider variations in the plate oscillations with increase in M. At M = 0.857 the spectrum contains several main peaks; however, in this regime the oscillation amplitude is small, while the peaks themselves are fairly smeared. This allows us to argue that the oscillations represent a response to broadband excitation from the vibrations of the tunnel as a whole.

For M = 1.147 the oscillations build up somewhat, while the frequencies of the main oscillation components decrease. The peaks at frequencies 190, 260, 345, 365, 405, and 525 Hz stand out; they become sharper which indicates a reduction of the oscillation damping.

The same tendency continues at M = 1.167: the amplitude increases somewhat, while the frequencies decrease. The peaks at frequencies of 175, 230, 250, 340, 355, 400, and 515 Hz can be distinguished.

At M = 1.286 the oscillation amplitude increases sharply (Fig. 9a). The peaks in the spectrum become narrow and sharp and their frequencies decrease: 155, 200, 310, 390, and 485 Hz.

With increase in M from 1.286 to 1.298 the amplitude increases even stronger (Fig. 9a). The spectrum composition remains almost invariant, while the oscillation frequencies increase somewhat (by about 10 Hz).

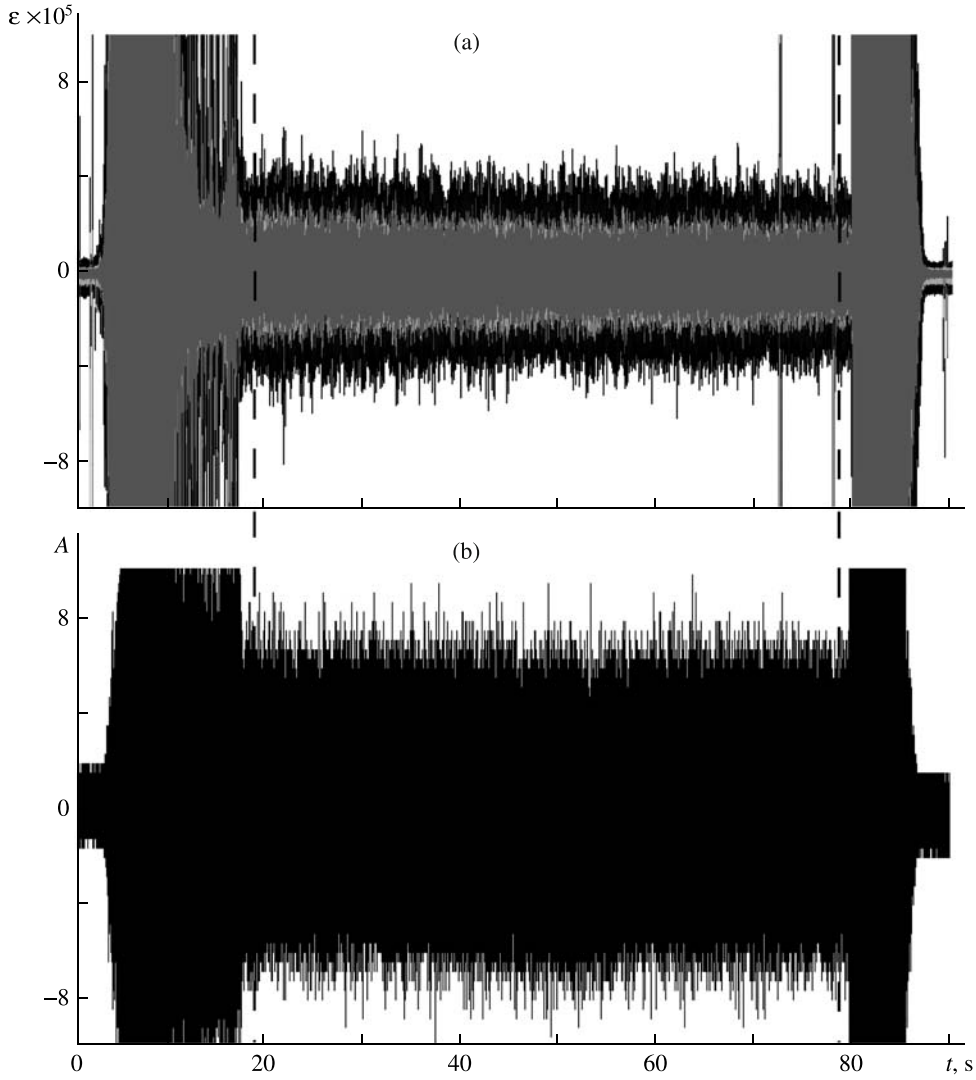

Fig. 12. Plate oscillations (a) and tunnel vibrations (b) during the third run. The stable M = 3.0 regime is separated by the broken lines.

An analysis of the bending amplitude distribution from the data of the pressure gages shows that the two lowest and most intense peaks in the spectra correspond to the (1, 1) and (2, 1) modes.

The strong growth of the oscillation amplitude starting from $M \approx 1.2$, the presence of five distinguishable sharp peaks the spectrum, of which two correspond to the predicted (1, 1) and (2, 1) modes (the other peaks cannot be uniquely identified), and the absence of convergence and coalescence of the peaks corresponding to the (1, 1) and (2, 1) modes, all these facts make it possible to argue that for $M > 1.2$ the plate is in the single-mode flutter range.

At the same time, there are some ambiguities in the experimental data. Judging from the theoretical results, the three peaks in the flutter spectrum, which could not be identified, represent the (2, 2), (3, 1), and (4, 1) modes. Apparently, the bending forms in the oscillations corresponding to these modes are distorted by residual stresses in the plate which remained after the welding and precisely for this reason cannot be identified.

Moreover, the behavior of the oscillation frequencies with increasing Mach number is also ambiguous. For $M = 0.857$ they are considerably higher than the natural frequencies determined on the stroke, they decrease with increase in the Mach number up to 1.286 and increase with further increase in M. This behavior can be attributed to the temperature effect: during the tunnel startup the plate is rapidly cooled and the fre-

quencies grow. Then the massive frame is also cooled, temperature stresses are reduced, and the frequencies also decrease. With increase in the Mach number the flow and then the plate are cooled even stronger and the frequencies increase again. However, this mechanism was not studied in detail.

Let us now consider the $M = 3.0$ regime (Fig. 12). During the oscillations the strain amplitude amounts to about 4.5×10^{-5} (cf. Fig. 9a), while the vibration amplitude is greater than in all transonic regimes. As before, the tunnel vibrations are of the type of broadband noise, without clearly expressed peaks. Thus, the vibrations that can excite plate oscillations are greater than in transonic regimes, whereas the plate response is weaker, so that at $M = 3$ flutter is not excited.

7. COMPARISON OF THE THEORETICAL AND EXPERIMENTAL DATA

As shown in Section 4, the most unstable modes, that is, excited at lower Mach numbers, are the $(1,\ 1)$ and $(2,\ 1)$ modes. This is in complete agreement with the experimentally obtained oscillation spectra, namely, the peak in the spectral range from 160 to 190 Hz corresponds to the $(1,\ 1)$ mode and that on the range from 200 to 260 Hz to the $(2,\ 1)$ mode.

The experimental boundary $(M)_{cr} \approx 1.2$ of the single-mode flutter range is close to the theoretical value $(M)_{cr} = \min\limits_{m,n} M_1(m,\ n) = 1.17$.

Unfortunately, the modes corresponding to the other peaks in the spectrum were not identified. This is due to eigenmode distortion caused by residual stresses that remained in the plate after welding. The theoretical results allow one to suggest that the unidentified peaks (Figs. 10 and 11) correspond to the other unstable modes.

At the same time, the conclusions made from our experimental results are unaffected by the residual stresses and the eigenmode distortion . Firstly, the $(1,\ 1)$ and $(2,\ 1)$ modes are distorted only slightly and this distortion has no effect on the flutter excitation mechanism [13]. Secondly, all the conclusions were made only by analyzing the experimental data: the theoretical results were not used in the data processing, while the analysis consisted in the investigation of the vibration types with successive elimination of their possible causes listed in Section 1.

Summary. The single-mode panel flutter in supersonic air flow was experimentally investigated for the first time. The experimental model included a plate which, starting from low supersonic Mach numbers ($M = 1.2$) may be subjected to the single-mode flutter, though the classical, coupled-type flutter cannot arise in it.

The experiments were carried out on the $0.8 < M < 1.3$ range and for $M = 3$. It is shown that for $1.2 < M < 1.3$ the plate is on the single-mode flutter range. In the experiments with $M = 3$ flutter was not detected. The results obtained in all the regimes are in good agreement with the theory: in the parameter space the boundaries of the flutter range, as well as the oscillation modes excited, agree with those obtained in the experiments.

The authors wish to thank S.N. Barannikov for assistance in carrying out the experiments, P.V. Makarov and A.V. Aref'ev for assistance in the work with the strain-measuring equipment, and K.A. Zhidyaev for discussion of the problems related with the numerical modeling of plate oscillations with account for the presence of the cavity.

The study was carried out with the partial support of the Russian Foundation for Basic Research (project No. 08-01-00618), grant MK-2313.2009.1, and the Program for the Support of Leading Science Schools (project NSh-1959.2008.1).

REFERENCES

1. V.V. Bolotin, *Nonconservative Problems of the Theory of Elastic Stability*, Pergamon (1963).
2. H.C. Nelson and H.J. Cunnigham, "Theoretical Investigation of Flutter of Two-Dimensional Flat Panels with One Surface Exposed to Supersonic Potential Flow," NACA Report No. 1280 (1956).
3. Dong Min-de, "Stability of an Elastic Plate in Supersonic Flow," Dokl. Akad. Nauk SSSR **120**, 726 (1958).
4. E.H. Dowell, "Nonlinear Oscillations of Fluttering Plate," AIAA J. **5**, 1856 (1967).
5. E.H. Dowell, "Generalized Aerodynamic Forces on a Flexible Plate Undergoing Transient Motion in a Shear Flow with an Application to Panel Flutter," AIAA J. **9**, 834 (1971).
6. E.H. Dowell, *Aeroelasticity of Plates and Shells*, Noordhoff, Leyden (1975).
7. T.Y. Yang, "Flutter of Flat Finite Element Panels in Supersonic Potential Flow," AIAA J. **13**, 1502 (1975).
8. Dong Min-de, "Eigenvalue Problem for Integro-Differential Equation of Supersonic Panel Flutter," Appl. Math. Mech. **5**, 1029 (1984).
9. O.O. Bendiksen and C.A. Davis, "Nonlinear Traveling Wave Flutter of Panels in Transonic Flow," AIAA Paper No. 1486 (1995).
10. O.O. Bendiksen and G. Seber, "Fluid-Structure Interactions with Both Structural and Fluid Nonlinearities," J. Sound Vibr. **315**, 664 (2008).
11. V.V. Vedeneev, "Flutter of a Wide Strip Plate in a Supersonic Gas Flow," Fluid Dynamics **40**(5), 805 (2005).
12. V.V. Vedeneev, "High-Frequency Plate Flutter," Fluid Dynamics **41**(2), 313 (2006).
13. V.V. Vedeneev, "High-Frequency Flutter of a Rectangular Plate," Fluid Dynamics **41**(4), 641 (2006).
14. V.V. Vedeneev, "Nonlinear High-Frequency Flutter of a Plate," Fluid Dynamics **42**(5), 858 (2007).
15. V.V. Vedeneev, "Numerical Investigation of Supersonic Plate Flutter Using the Exact Aerodynamic Theory," Fluid Dynamics **44**(2), 314 (2009).
16. A.A. Movchan, "Stability of a Panel in Motion in a Gas," Prikl. Mat. Mekh. **21**, 231 (1957).